

## Final report on project

“Photosynthetic reaction centers/carbon nanotubes hybrid systems” (OTKA PD 116739)

Dr. Kata Hajdu

### Introduction

The project focused on the fabrication of hybrid photoactive bio-nanocomposites based on different conductive and semiconductive, principally carbon based materials, like carbon nanotubes and graphene sheets. Light harvesting process of the composites was provided by photoactive biological entities. In particular, photosynthetic reaction center proteins (RCs) are of special interest, due to their exceptionally high quantum yield of energy conversion. One of the first steps of photosynthesis takes place in the RCs. These pigment–protein complexes are integrated in the photosynthetic membranes of plant and photosynthetic bacterial cells. The energy of every absorbed photon results in the separation of positive and negative charges:  $P^+BPheo^-$  state is followed by the  $P^+Q_A^-$  state, where  $P^+$  is the oxidized primary electron donor, a specialized bacteriochlorophyll dimer,  $(BChl)_2$ .  $BPheo$  is the first electron acceptor, a monomer bacteriopheophytine, and  $Q_A^-$  is the reduced quinone-type primary electron acceptor. The separated charges are then further stabilized in the form of the  $P^+Q_B^-$  redox state, where  $Q_B^-$  is the reduced secondary quinone. Combining RCs with conductive or semiconductive carriers, direct redox interactions can take place in the hybrid composites. RCs purified from *Rhodobacter (Rb.) sphaeroides* purple bacteria were bound physically and chemically to different carbon-based materials like CNTs (non-functionalised, carboxyl-functionalised and amine-functionalised multiwalled carbon nanotubes), graphene sheets and also to porous silicon (PSi) wafers.

### Carbon nanotubes

The main concept of the project was the preparation of photoactive biocomposites by the application of carbon nanotubes as conductive carriers of the RC. Different carbon nanotubes and immobilisation techniques were used in order to bind the RC efficiently to the conductive surface.

RC was bound to multiwalled carbon nanotubes through physical and chemical binding. Chemical binding to carboxyl-functionalised multiwalled carbon nanotubes was accomplished through the cross linker molecule called carbodiimide and succinimide, specific crosslinkers to carboxyl groups. This way RC was immobilised through one of its carboxyl groups. On the amine-functionalised CNT surface, the applied crosslinker was glutaraldehyde (GTA) which connects the available amine groups of the CNT and the RC.

#### Binding efficiency (Szabó *et al.*, *Radiocarbon*, 2018)

Efficiency of the binding procedures is usually verified by different microscopic and spectroscopic techniques. Scanning Electron Microscopy (SEM), Energy-Dispersive X-ray Spectroscopy (EDX) and Atomic Force Microscopy (AFM) was applied in order to record the RC bound on to the surfaces. Apart of these characterisation techniques, we introduced a new method during this project for the determination of the bound RCs on the CNT surface. Isotope analytical characterization of carbon based nanocomposites was carried out in order to determine the exact amount of immobilized RC on carbon nanotubes and demonstrate the binding efficiency of the used immobilization techniques. Carbon source of the RC is supplied by the Siström-medium which is a complete growth medium for photo-heterotrophic growth of the photosynthetic bacteria. In addition to the carbon content of potassium-succinate (the main carbon source of this medium) the recent atmospheric carbon-dioxide (around 100 pMC) as secondary source can also influence the radiocarbon content of the bacterium cells. The isotope constitution of biohybrid materials prepared from bare and/or doped carrier CNTs and enzymes proved that isotope analytics is a useful tool for determining the quantitative binding of the biological materials to the carrier matrices. After determining the quantitative amount of the enzyme, specific activity of the sample can be determined.

#### Photoactivity

Kinetic absorption change (flash photolysis) measurements were done by an in-house single-beam kinetic spectrophotometer so as to define the characteristics of the light induced charge recombination in the RC after the immobilisation. The stabilized light of 55 W halogene lamp was passed through a Joben Yvon monochromator and the sample. Excitation was achieved by a xenon flash lamp (type EG&G FX200,  $t_{1/2} \approx 8.5$  ms). The decay kinetics was decomposed assuming two exponential components of which the lifetime and the

contribution were analyzed. The fast component is generally assigned to  $P^+Q_A^- / PQ_A$  charge recombination since the lifetime of the slow component is attributed to the  $P^+Q_B^-/PQ_B$  charge recombination.

#### Electric properties (Szabó *et al.*, *Photosynthesis Research*, 2017)

A home-made electrochemical cell with three electrodes was designed and fabricated. RCs were chemically bound to the ITO surface through functionalized MWCNTs with different crosslinkers. Carboxyl-functionalized MWCNTs were activated by the mixture of N-cyclohexyl-N0-(2-morpholino-ethyl)-carbodiimide methyl-p-toluene-sulfonate (EDC) and N-hydroxy-succinimide (NHS, Sigma-Aldrich), while the surface of ITO was silanized by 3-aminopropyl-triethoxysilane (APTES). Finally, the activated MWCNTs were bound to the surface treated ITO by EDC-NHS. ITO covered by RC samples served as the working electrode, since the counter and the reference electrodes were platinum and Ag/AgCl, respectively. 2,3-Dimethoxy-5-methyl-1,4-benzoquinone (UQ-0, Sigma) and ferrocene were used as mediators. Light-induced changes in the cell were measured using a Metrohm PGSTAT204 type potentiostat/galvanostat at ambient temperature. Sample was illuminated by white light of 150 W slide projector halogen lamp through a fiber optical guide. The incident light intensity was 78 mW cm<sup>-2</sup>. The pH was adjusted to 8.0 by the addition of TRIS buffer. Photocurrent was generated in the RC-sensitized cell and was blocked by different concentrations of terbutryn or o-phenanthroline (electron transport inhibitors, which bind specifically to the secondary quinone acceptor site of the RC).

In order to measure the herbicide inhibition in real time (binding/unbinding of the herbicides to/from the functionalized electrode, regeneration of the electrodes), a polydimethyl-siloxane-based microfluidic device with an integrated microelectrode system was constructed with an electrode arrangements similar to the traditional electrochemical cell. The ITO/RC working electrode was prepared in advance the same way as for the conventional cell, and the electrodes were assembled into the polymer chamber. The volume of the microfluidic chamber was 300  $\mu$ L, and the distance between the working and counter electrodes was approximately 2 mm. The alternating flow of the reference medium versus the reaction mixture supplemented with the inhibitor (terbutryn or o-phenanthroline) was regulated by a mechanical control valve. The flow rate was 0.5 mL/min.

We were able to measure photocurrents comparable to those published in the literature. The current was sensitive to photosynthetic inhibitors terbutryn and o-Phe. By building a microfluidic cell, we managed to reduce the sample volume to 300  $\mu\text{L}$ . The flow cell also allowed the regeneration of the herbicide sensor, by washing the cell with the reaction medium containing excess amounts of UQ-0, allowing its successive use in real time. Thus, this device might be suited to determine the kinetic parameters of binding/unbinding of different inhibitor and cofactor molecules at the secondary quinone acceptor site of the RC.

#### Singlet oxygen formation (Hajdu et al., Materials, 2017)

RC purified from *Rhodobacter sphaeroides* purple bacteria was immobilized on multiwalled carbon nanotubes (CNTs). Carboxyl – and amine-functionalised CNTs were used, so different binding procedures - physisorption and chemisorption as well - could be applied as immobilization techniques. Light-induced singlet oxygen production was measured in the prepared photoactive biocomposites in water-based suspension. Singlet oxygen concentration was determined by His-mediated chemical trapping measuring oxygen uptake with a Hansatech DW2/2 Clark type electrode. The effect of carbon nanotubes was detected in mixed samples, and also after immobilizing the RC on the MWCNT surface with physical sorption or chemical binding, as described above.

It has been shown that carbon nanotubes reacted with and quenched the uprising, highly reactive singlet oxygen. The distance between RCs and MWCNTs is determining factor in point of quenching efficiency, most probably due to the diffusion path. The biggest quenching effect was visible after physical sorption, where RC is bound directly on the MWCNT surface, without any crosslinker bridges. In the case of mixed samples, the quenching effect was smaller due to the larger distance between the interacting components and also because of the micelle system which is necessary to keep the system stable in the water phase.

$^1\text{O}_2$  quenching proceeds in physical and chemical ways, and both of these mechanisms has to be considered in case of carbon nanotubes. We made an attempt to clarify which mechanism is preferable in the MWCNT/RC systems, so that measurements were done with and without chemical trapping of  $^1\text{O}_2$  by histidine. Histidine traps the  $^1\text{O}_2$  chemically, so this experimental arrangement represents notably the chemical way of quenching mechanisms. Measurements showed considerable difference - in the absence of histidine smaller change was detected compared to the equilibration oxygen concentration. In addition, positive turn in the oxygen concentration change was recorded. It is reasonable to assume, that MWCNT

quenched the  $^1\text{O}_2$  preferentially through chemical interaction under our experimental conditions.

Beyond the quenching, another effect was found for both types of functionalized MWCNT (MWCNT-COOH and MWCNT-NH<sub>2</sub>) samples. Positive change was found in the O<sub>2</sub> concentration showing the increase of oxygen content in the electrode environment. The possible sources of the “extra O<sub>2</sub>” are functional groups on the surface of the MWCNT, mostly in case of MWCNT-COOH where the functionalisation procedure requires a highly oxidative environment. These oxygenic groups can split to O<sub>2</sub> upon light excitation, and synproportionation with the uprising  $^1\text{O}_2$  has to be also considered.

Hydrogen peroxidase (*Magyar et al, Journal of Nanomaterials, 2016*)

Based on our experiences on RCs another redox protein, hydrogen peroxidase (horse radish peroxidase, HRP) was bound to electrode surfaces through carbon nanotubes. We found that HRP keeps its enzyme activity after the binding and the H<sub>2</sub>O<sub>2</sub> concentration can be determined in real time with high sensitivity. The system we designed can be used as a model for a specific and high sensitivity biosensor application for detecting H<sub>2</sub>O<sub>2</sub>.

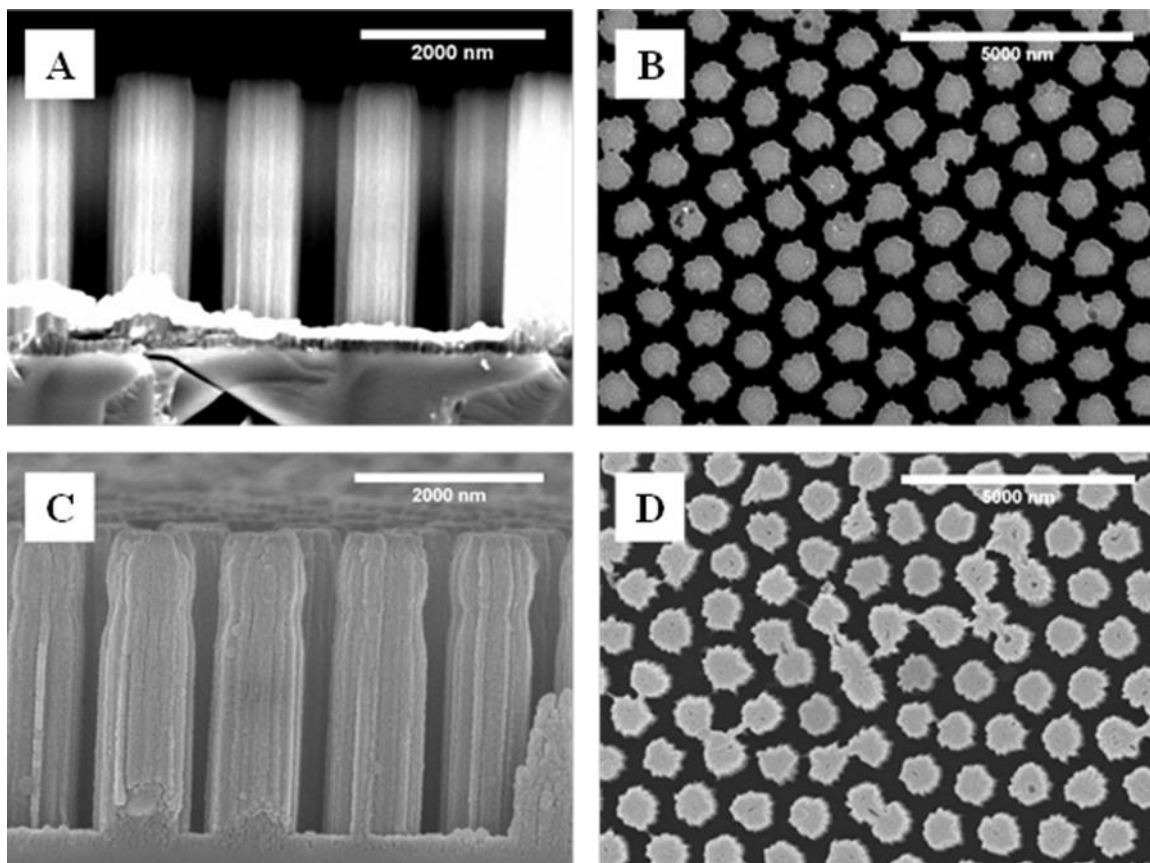
## **Graphene**

Since its discovery, graphene has attracted intense attention of researchers for its broad range of potential applications. In contrast to the “quasi-1D” carbon nanotubes, 2D films have been introduced as more suitable building blocks for new types of applications in mechanically flexible and stretchable, optically transparent electronic systems. In order to create a functional bio-nanocomposite material, we combined photosynthetic reaction center proteins (RCs), purified from purple bacteria, with graphene prepared by liquid exfoliation method. We measured and compared the light-induced changes in the conductivity of the bare graphene multilayer and the RC/graphene-film composite - using 808 nm diode-laser (DL) excitation, eliciting charge separation in the RC protein complex. With RCs deposited on the surface of the graphene film, a ca. 100 ohm resistance change was measured, which depended on the DL-light intensity, pulse length and frequency. The electrical conductivity under light excitation depended on the intrinsic conductivity of the individual layers and on structural features, in particular on the spatial arrangement and interconnections of layers.

## **Porous silicon**

Silicon has been applied as biosensor since the very beginning of the biosensing technology. After the discovery of porous silicon (PSi) and recognising its unique optical properties, new prospects were revealed in the area of sensing and biosensing. 2D PSi structures can be easily fabricated by metal assisted chemical etching (MACE), a chemical etching reaction that dissolves silicon using an oxidising agent and a metal as catalyst. In addition to a controllable and high exposed surface area that may be decorated with a functional material, PSi pillar (PSiP) structures have been demonstrated to be useful in the optical detection of chemical analytes.

PSiP/RC composites were fabricated by the immobilization of RC on the PSiP surface. First, electrochemical polymerisation of aniline took place in an electrochemical cell with three-electrode arrangement, where the working, counter and reference electrode was PSiP, platinum and Ag/AgCl, respectively. A 0.25 M concentration of aniline was dissolved in 0.5 M HCl solution. Voltage was sweeping between 0 V - 1.7 V and number of stop-crossings were 4. Glutaraldehyde (GTA) in 2.5% concentration served as an amine-targeted crosslinker between the PANI-covered silicon surface and the RC. The surface was dipped in the GTA solution for 15 minutes, washed with phosphate buffer and dried under the stream of nitrogen. After the primary functionalization, the samples were incubated in 11  $\mu$ M of RC for 2 hours at 4 °C, followed by rinsing with phosphate buffer and drying under the stream of nitrogen.



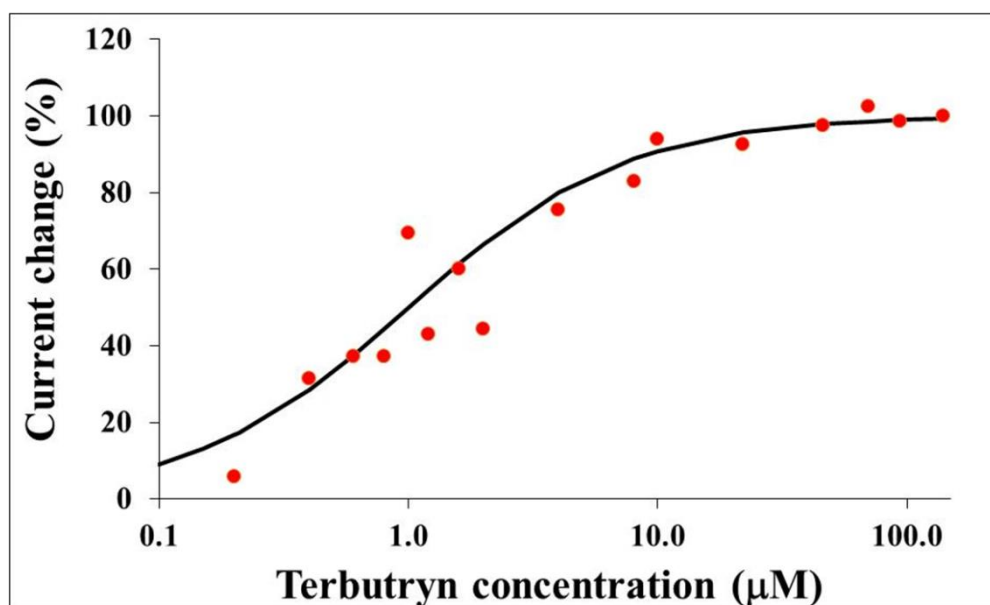
SEM images of PSiP structures. (A) Transversal and (B) superficial view before and (C) transversal and (D) superficial view after PANI deposition, respectively.

PSiP/RC working electrodes were prepared by a laminating procedure. A copper wire, as an electrical contact, was fixed on the non-porous part of the PSiP plate with the use of conductive carbon paste (derived from SUPELCO). The electrodes were covered by a laminating foil. As a result of the lamination, only a circular patch of the porous surface was in contact with the electrolyte solution (10 mM phosphate buffer, pH: 7.0). The approximate diameter of the available porous silicon surface was 6 mm that corresponds to 28.5 mm<sup>2</sup> surface area.

Successful immobilization of photosynthetic bacterial reaction centre (RC) was performed on PANI covered porous silicon pillar structure (PSiP). With respect to the reference structure without PANI coverage, the magnitude of the visible light induced photocurrent measured on PSiP was found to improve significantly after the controlled electrodeposition of the conducting polymer in the presence of added quinone. Further enhancement of the photocurrent was achieved by the immobilization of RC. Direct redox connection was found between the RC and the carrier matrix since the RC-functionalised composites showed increased photocurrent even without adding any redox component to the electrolyte, revealing

a redox interaction between the RC and the PSiP after light-excitation and hence, causing a change in the charge state of the electrode surface and inducing current flow in the electrochemical cell.

Due to the presence of specific redox cofactors and binding sites of the RCs, the photocurrent of the biocomposite device is found to be sensitive to specific herbicides such as terbutryn, as a result of its interaction with RC acceptor site.



Level of inhibition given in percentage, in the function of terbutryn concentration in logarithmic representation. Electrolyte consisted of 100 µM UQ-0 and 10 mM phosphate buffer (pH: 7.0). Solid line was calculated by the fitted  $I_{50}=1.19 \mu\text{M}$  ( $SD=0.7 \mu\text{M}$ ).

RC/PSiP biocomposite device has been demonstrated as an electrochemical biosensor for the detection of herbicides. Photocurrent measurements performed under different terbutryn concentrations revealed the apparent inhibitor dissociation constant,  $I_{50}=1.19\pm 0.7 \mu\text{M}$  with the limit of detection of  $0.08 \mu\text{M}$  for terbutryn. Such sensitive and selective systems can be further developed by reducing the measured sample quantity, e.g. in a microfluidic cell.

### **Related publications:**

Hajdu, K., Balderas, R.F., Agarwal, V., Carlino, A., Nagy, L. (2018) Silicon-based photoactive biocomposites for electrochemical biosensing, *Sensors and Actuators B.*, (Under revision)

Szabó, T., Janovics, R, Túri, M., Futó, I., Papp, I., Braun, M., Németh, K., Szekeres, G.P., Kinka, A., Szabó, A., Hernádi, K., Hajdu, K., Nagy, L., Rinyu, L. (2018) Isotope analytical characterization of carbon based nanocomposites, *Radiocarbon*, DOI: 10.1017/RDC.2018.63

Hajdu, K., Ur Rehman, A., Vass, I., Nagy, L. (2017) Detection of Singlet Oxygen Formation inside Photoactive Biohybrid Composite Material, *Materials*, DOI: 10.3390/ma11010028.

Hajdu, K., Szabó, T., Sarrai, A.E., Rinyu, L., Nagy, L. (2017) Functional nanohybrid materials from photosynthetic reaction center proteins, *International Journal of Photoenergy*, DOI: 10.1155/2017/9128291

Szabó, T., Csekő, R., Hajdu, K., Nagy, K., Sipos, O., Galajda, P., Gyöző, G., Nagy, L. (2016) Sensing photosynthetic herbicides in an electrochemical flow cell, *Photosynthesis Research*, DOI: 10.1007/s11120-016-0314-2

Magyar, M., Rinyu, L., Janovics, R., Berki, P., Hernádi, K., Hajdu, K., Szabó, T., Nagy, L. (2016) Real-Time Sensing of Hydrogen Peroxide byITO/MWCNT/Horseradish Peroxidase Enzyme Electrode, *Journal of Nanomaterials*, 3:1-11.

Szabó, T., Magyar, M., Hajdu, K., Dorogi, M., Nyerki, E., Tóth, T., Lingvay, M., Garab, Gy., Hernádi, K., Nagy, L. (2015) Structural and Functional Hierarchy in Photosynthetic Energy Conversion—from Molecules to Nanostructures, *Nanoscale Res. Letters*, 10:458 DOI 10.1186/s11671-015-1173-z

### **Related talks and poster presentations:**

Hajdu, K., Kinka, A., Rehman, A.U., Vass, I., Nagy, L. (2016) Detection of light induced singlet oxygen generated by bacterial reaction center, Regional Biophysics Conference, Triest, Italy

Hajdu, K., Agarwal, V., Gergely, Cs., Palestino, G., Marquez, J., Zimányi, L., Nagy, L. (2016) Light induced redox interaction in photosynthetic reaction center/porous silicon hybrid materials, Porous Semiconductors – Science and Technology, Tarragona, Spain

Hajdu, K., Balderas, R.F., Agarwal, V., Pacholski, C., Nagy, L. (2017) Photoactive electrodes based on photosynthetic bionanocomposites, 5th International Conference on Bio-Sensing Technology, Riva del Garda, Italy

Szabó, T., Tomashevich, T., Panajotović, R., Vujin, J., Sarrai, A.E., Váró, Gy., Szegletes, Zs., Garab, Gy., Hajdu, K., Nagy, L. (2017) Photosynthetic reaction-center/graphene biohybrid for optoelectronics, 5th International Conference on Bio-Sensing Technology, Riva del Garda, Italy

Hajdu, K., Balderas, R.F., Agarwal, V., Pacholski, C., Nagy, L. (2018) Photoactive hybrid bio-nanocomposites based on photosynthetic bacterial reaction center, Porous Semiconductors - Science and Technology 2018, La Grande Motte, France